QUANTUM EXCITATIONS IN MAGNETIC CLUSTERS

NORDAL CAVADINI

Abstract. The microscopic magnetic properties in solids are the results of true quantum mechanical interactions between the electrons. After a brief introduction, basic model predictions are developed for dimer clusters, and presented in the context of inelastic neutron scattering investigations. It is explained how the relevant microscopic information is extracted from the experimental outcomes.

1. Introduction

The microscopic understanding of the magnetic properties in matter remains a central issue in solid state physics. The phenomenological formulation of magnetic interactions in terms of quantum mechanical exchange - originally developed to account for spin correlations in ionic solids - has been successfully applied to a large variety of magnetic systems, and still constitues the effective approach used to characterize new and unconventional compounds. Among these, low dimensional spin 1/2 magnetic insulators continue to attract considerable scientific interest, both from the theoretical and from the experimental point of view, because of their deep connection with the still unsolved issue of high–T_c superconducting materials [1]. The natural link between model predictions and actual behaviour of a given magnetic system is provided by the experiment. The more demanding the requested characterization is, the more comprehensive the experimental investigation has to be. In this respect, neutron scattering spectroscopy has established itself as the cleanest and the most conclusive technique at disposal, often yielding cutting–edge results which trigger additional theoretical efforts. It is the scope of this contribution to brefly review to the non specialist how our knowledge of the microscopic magnetic interactions has progressed, and which unique experimental evidences neutron scattering can provide. The discussion will be exemplified by presenting selected results from simple, yet nontrivial quantum spin systems: Isolated and quasi–isolated magnetic clusters.

Nordal Cavadini, Laboratory for Neutron Scattering, ETH Zürich & Paul Scherrer Institut, CH–5232 Villigen PSI, Switzerland (e–mail: Nordal.Cavadini@psi.ch).

2. A BRIEF REVIEW

From the early recognition that magnetism in ionic solids is connected with unpaired valence electrons, only the quantum revolution at the beginning of the 20th century established the phenomenological framework which is still in use to model magnetic interactions. Introduced by Heisenberg in 1926 [2], the spin exchange model was put into operator form by Dirac [3] and van Vleck [4] soon thereafter. At the heart of the model, the spin S of the electron as an additional degree of freedom which encodes the effective interaction between pairs of magnetic ions. This interaction is of quantum mechanical nature, being a consequence of electronic orbital overlap (exchange), and is expressed by the exchange coupling constant J after

$$H_{spin} = -J\ \hat{S}_1 \cdot \hat{S}_2 \tag{2.1}$$

In the above formalism, $\hat{S}_1$ and $\hat{S}_2$ represent the spin operators for the localized magnetic ions sitting at sites C_1 and C_2 in the solid, respectively. The sign of the constant J provides the nature of the magnetic interaction $C_1 \leftrightarrow C_2$, the strength $|J|$ fixes the according energy scale. For instance a positive J applies to ferromagnetic coupling, the tendency of neighboring spins to align parallel to each other in order to minimize the exchange energy in equation 2.1. This configuration will be stable against thermal disturbances provided $k_B T \ll |J|$. $\hat{S}$ itself is related to the classical magnetic moment m by the Bohr magneton μ_B, the quantum of magnetic moment [1] . In the case of free electrons it holds

$$m_i = -2\ \mu_B < \hat{S}_i > \tag{2.2}$$

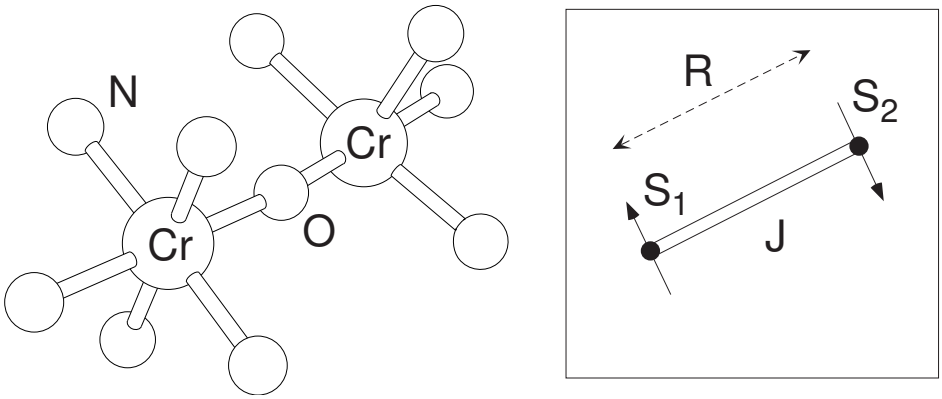

FIGURE 1. Left, schematic view of the acid rhodo complex. Right, sketch of the antiferromagnetic exchange interaction J between spin S_1 and spin S_2 sitting at the chromium places (separation R), as explained in text.

Originally introduced to account for the direct ferromagnetic interaction between pairs of well–localized magnetic centers ($C_1 \leftrightarrow C_2$), the Heisenberg spin exchange model was extended by Anderson to include indirect interactions through a ligand L ($C_1 \leftrightarrow L \leftrightarrow C_2$)

[1] $1\ \mu_B = \frac{e\hbar}{2m_e} \sim 9.274 \cdot 10^{-24}\ \mathrm{Am}^2$

[5] - an example is proposed in Figure 1. This superexchange mechanism is much more common than the direct exchange, and in the majority of the cases antiferromagnetic (AF), expressing the tendency of the moments to microscopically align antiparallel to each other - a postulation which goes back to the pioneering work of Néel and van Vleck (see [5], [6] and references therein). AF structures are elusive, since the individual moments compensate each other on a macroscopic scale. They can however be investigated on a microscopic scale. Among the first successes of neutron scattering on the subject, we recall the direct experimental determination of several three–dimensional antiferromagnetic structures by Wollan and collaborators [7], [8].

For our convenience, in the following we will not consider extended magnetic systems but rather focus our attention on the limit of isolated clusters, which have the advantage to be easily amenable to analytical expressions. The simplest, yet nontrivial cluster is the AF dimer composed by two coupled spins, each having $S = 1/2$. The quantization conditions on S impose that each of the two spins can either assume the spin state up $|\uparrow\rangle$ or the spin state down $|\downarrow\rangle$, yielding in total 4 possible dimer configurations (see Table 1).

spin	state	energy
$S = 1$	$\|\uparrow\uparrow\rangle$	$+\frac{1}{4}\|J\|$
$S = 1$	$\frac{1}{\sqrt{2}}\{\ \|\uparrow\downarrow\rangle + \|\downarrow\uparrow\rangle\ \}$	$+\frac{1}{4}\|J\|$
$S = 1$	$\|\downarrow\downarrow\rangle$	$+\frac{1}{4}\|J\|$
$S = 0$	$\frac{1}{\sqrt{2}}\{\ \|\uparrow\downarrow\rangle - \|\downarrow\uparrow\rangle\ \}$	$-\frac{3}{4}\|J\|$

TABLE 1. Configurations and energy levels of a $S = 1/2$ antiferromagnetic dimer cluster, as introduced in the text. Inelastic neutron scattering at the lowest temperature causes transitions from the $S = 0$ ground state to the $S = 1$ excited states. The energy needed to excite the dimer $(+|J|)$ is supplied by the neutron.

The spectrum of H_{spin} favours in the AF case a $S = 0$ singlet ground state, separated by an energy $|J|$ from three degenerate $S = 1$ triplet states. These configurations correspond to the eigenvectors of equation 2.1 restricted to the four–dimensional space spanned by the spin pair - the coherent superposition of the classical solutions $|\uparrow\downarrow\rangle$ and $|\downarrow\uparrow\rangle$ is the result of the quantum fluctuations demanded by the uncertainity principle.

3. NEUTRON SPECTROSCOPY

Along the lines of the above discussion, a complete experimental investigation will be generally required to determine the exchange coupling constant J of the magnetic system,

as well as the resulting microscopic spin–spin correlations. In the dimer case, this implies the measurement of the excitation energy gap $E_1 - E_0$ between the $S = 1$ triplet and the $S = 0$ singlet, as well as the quantitative determination of the transition matrix element $S = 0 \rightarrow S = 1$ connecting these states. Neutron scattering, a diffractive technique matched to the time and space scales of magnetic interactions, turns out to be the experimental method of choice. Its advantages rely in the possibility to control both the energy transfer $\hbar\omega$ and the momentum transfer $\hbar\vec{\kappa}$ from the neutron to the sample during the interaction. The magnetic interaction itself, mediated by the spin of the neutron, is clean, well–understood and nondestructive - issues which promote neutron scattering at the forefront of particle research in solid state physics, see ref. [9] for an introduction.

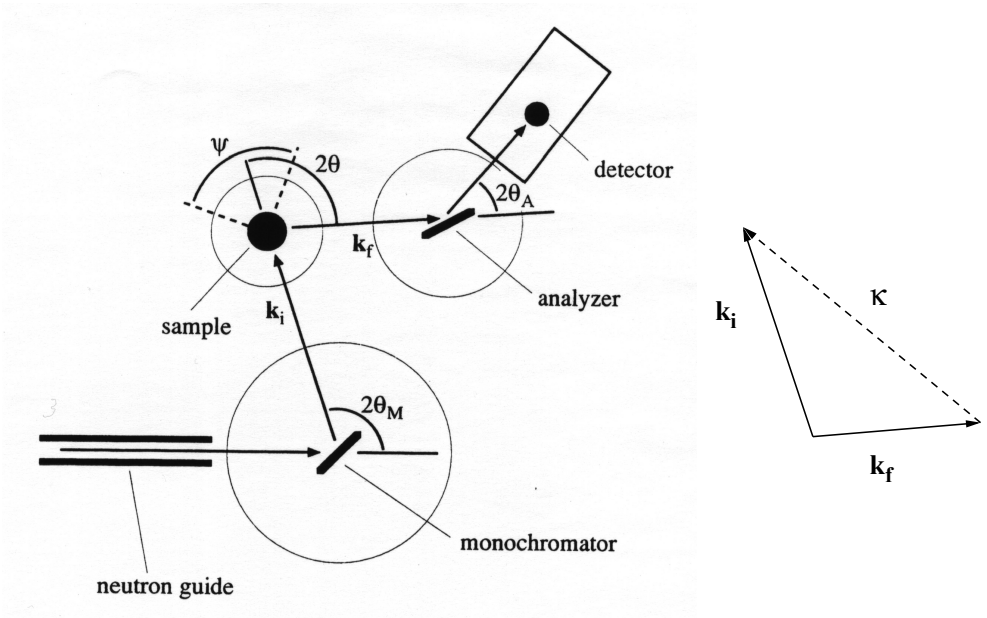

FIGURE 2. A typical neutron three–axis spectrometer. Energy and momentum transfer $\{\hbar\omega,\ \hbar\vec{\kappa}\}$ to the sample can be selectively controlled by the incoming and outcoming neutrons k_i and k_f, respectively, allowing the complete investigation of time and space correlations. On the right, the scattering triangle corresponding to equation 3.1 in the text.

Referring to Figure 2, the following relations hold

$$\hbar\omega = \frac{\hbar^2}{2m_n}(k_i^2 - k_f^2) \qquad \vec{\kappa} = \vec{k}_i - \vec{k}_f \tag{3.1}$$

where m_n stands for the mass of the neutron, and the indices i, f refer to initial and final neutron states, respectively. In the case of isolated clusters, investigations are usually performed with a powder sample, which allows to collect integrated information. The expected scattering cross section for a $S = 0 \rightarrow S = 1$ dimer transition at the lowest temperature reads

$$\frac{d\sigma}{d\Omega d\omega}(\kappa,\omega) \sim |f(\kappa)|^2 \ (1 - \frac{\sin(\kappa R)}{\kappa R}) \ \delta(\hbar\omega - (E_1 - E_0)) \tag{3.2}$$

where $\hbar\kappa$, $\hbar\omega$ denote the modulus of the momentum and the energy, respectively as defined in equation 3.1, and R the distance between the single spins within the dimers (Figure 1). The squared magnetic form factor $|f(\kappa)|^2$ is a known ionic–specific quantity, which monotonically decreases in κ. Equation 3.2 contains two pieces of information: Firstly, the energy part

$$\delta(\hbar\omega - (E_1 - E_0)) \tag{3.3}$$

which is peaked at the singlet–triplet excitation energy, corresponding to the exchange coupling constant $|J|$ in the system, after Table 1. Secondly, the structural part proportional to

$$(1 - \frac{\sin(\kappa R)}{\kappa R}) \tag{3.4}$$

which is modulated by the distance R of the moments within the dimer, yielding direct evidence of the spins involved in the exchange. Under the conditions discussed above, equation 3.2 holds not only for a $S = 1/2$ dimer cluster, but at arbitrary S.

In Figure 3, the outcome of neutron spectra from binuclear $S = 3/2$ Cr^{3+} dimers contained in acid rhodo chromium chloride are reproduced from ref. [10]. The measurements were performed varying the energy transfer $\hbar\omega$ at given constant momentum transfer $\hbar\kappa$ (Figure 2). The well–defined excitation observed at $\hbar\omega = E_1 - E_0 \sim 3.82$ meV [2] is indicative of the intradimer exchange coupling constant. The expected sharp δ transition is broadened by the finite resolution of the spectrometer, retaining however its symmetric shape. At the same time, the observed modulation of the integrated intensity (Figure 4) corresponds to the distance $R \sim 3.85$ Å, which separates pairs of Cr^{3+} ions, as determined from crystallographic investigations (Figure 1). The detailed microscopic characterization of dimers and molecular clusters in general constitutes a fundamental issue on its own right. Inelastic neutron scattering allows to gain deep insights into the microscopic mechanisms governig their magnetic interactions, see ref. [11] for a recent example.

There are cases where the magnetic interactions extend beyond the dimer cluster, albeit originating from the same physical picture discussed above. In this context, Figure 5 shows excitations profiles from the $S = 1/2$ Cu^{2+} dimer compound $KCuCl_3$. Opposite to the situation depicted in Figure 3, the spectral shapes in Figure 5 are no more resolution limited and rather depend upon the momentum transfer $\hbar\kappa$, indicating that the nature of the $S = 0 \rightarrow S = 1$ transitions is propagating. Excitations in $KCuCl_3$ do not remain localized to a given dimer, but are free to hop from one site to the other in the lattice, building triplet waves whose energy $\epsilon = E_1 - E_0$ above the ground state now depends on

[2] $1\ meV/k_B \sim 11.6K$

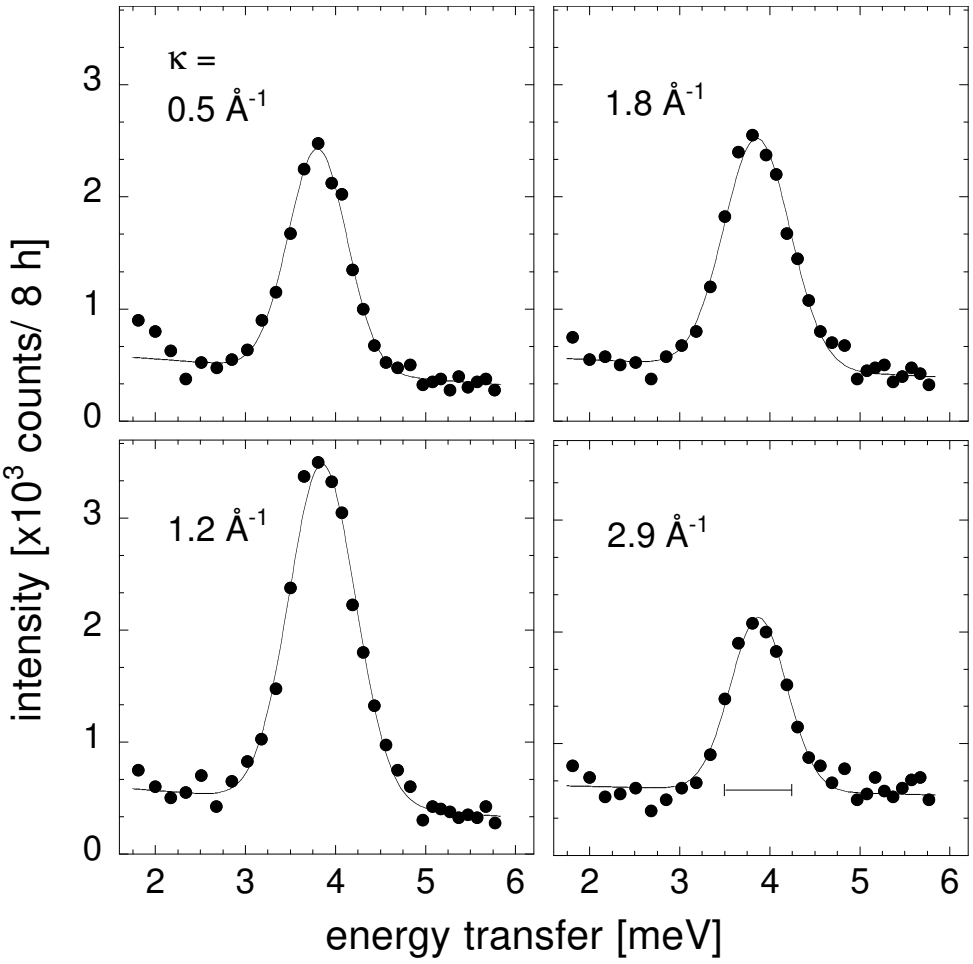

FIGURE 3. Observed profiles for the $S = 0 \to S = 1$ magnetic excitations in deuterated acid rhodo chromium chloride at $T \sim 4.2$ K (Figure 1). From the peak position on the energy scale, the exchange coupling constant is determined as $|J| \sim 3.82$ meV as explained in the text (cf. equation 3.2). The horizontal bar indicates the instrumental resolution.

the wavevector $\vec{\kappa}$. Figure 5 thus reproduces in a first approximation the density of states corresponding to

$$\frac{d\sigma}{d\Omega d\omega}(\kappa,\omega) \sim |f(\kappa)|^2 \, (1 - \frac{\sin(\kappa R)}{\kappa R}) \, \frac{1}{4\pi\kappa^2} \int \int_{|\vec{\kappa}|=\kappa} \delta(\hbar\omega - \epsilon(\vec{\kappa})) \tag{3.5}$$

These issues call for a more involved investigation: single crystals (opposite to powders) are necessary to selectively explore the energy dispersion relation $\epsilon(\vec{\kappa})$ along different crystallographic directions. The periodicity and the amplitude of the dispersion relation will then enable to determine the additional exchange couplings responsible for the hopping of the excitations. The intensity fit reproduced in Figure 5 is the *a posteriori* result expected

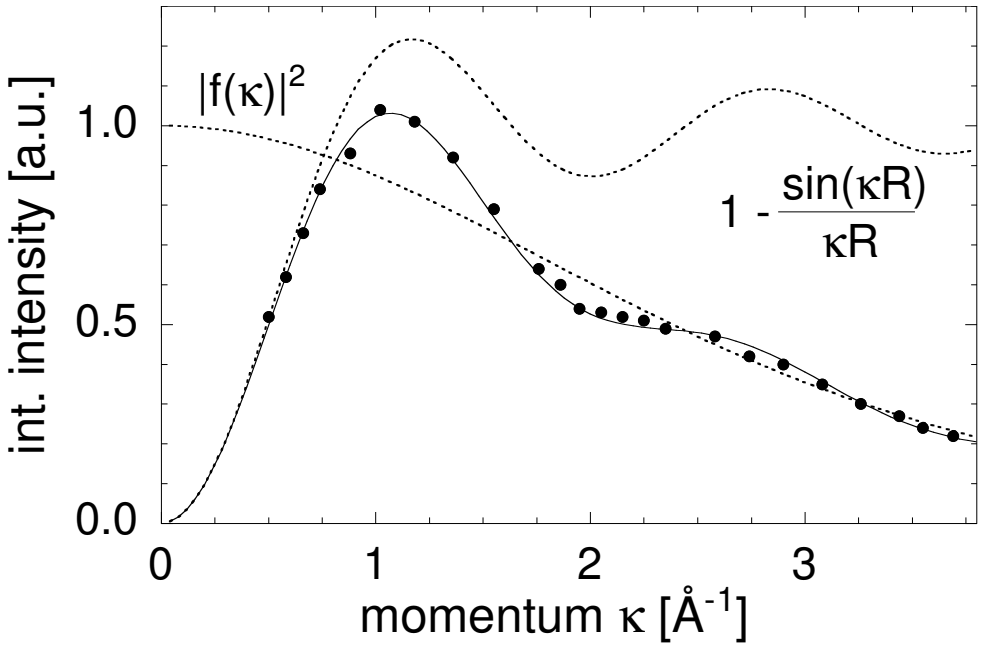

FIGURE 4. Normalized intensity for the $S = 0 \rightarrow S = 1$ magnetic excitations at $T \sim 4.2$ K, given by the area of the peaks in Figure 3. The characteristic oscillatory behaviour in κ depends on the distance R of the single spins S_1 and S_2 within the dimers, as explained in the text (cf. equation 3.2).

from the coupling scheme determined in single crystal investigations [12]. Generally, the observation of magnetic interactions which involve several dimer clusters implies a cross–over from the isolated two–body interaction of equation 2.1 to the much more complicated many–body limit described by

$$H_{spin} = -\frac{1}{2}\sum_{i,j} J_{ij}\ \hat{S}_i \cdot \hat{S}_j \tag{3.6}$$

where the summation runs over all pairs i, j of correlated spins. The challanges imposed by the above considerations on the theory and on the experiment will hopefully be addressed in a future contribution.

4. SUMMARY

Basic concepts behind microscopic magnetic interactions were briefly presented, along with selected examples from the field of magnetic excitations in finite clusters. In the dimer limit, model predictions have been compared to experimental results obtained with neutron scattering spectroscopy, a technique which plays the leading role in demanding magnetic investigations. The direct determination of exchange coupling constants and microscopic

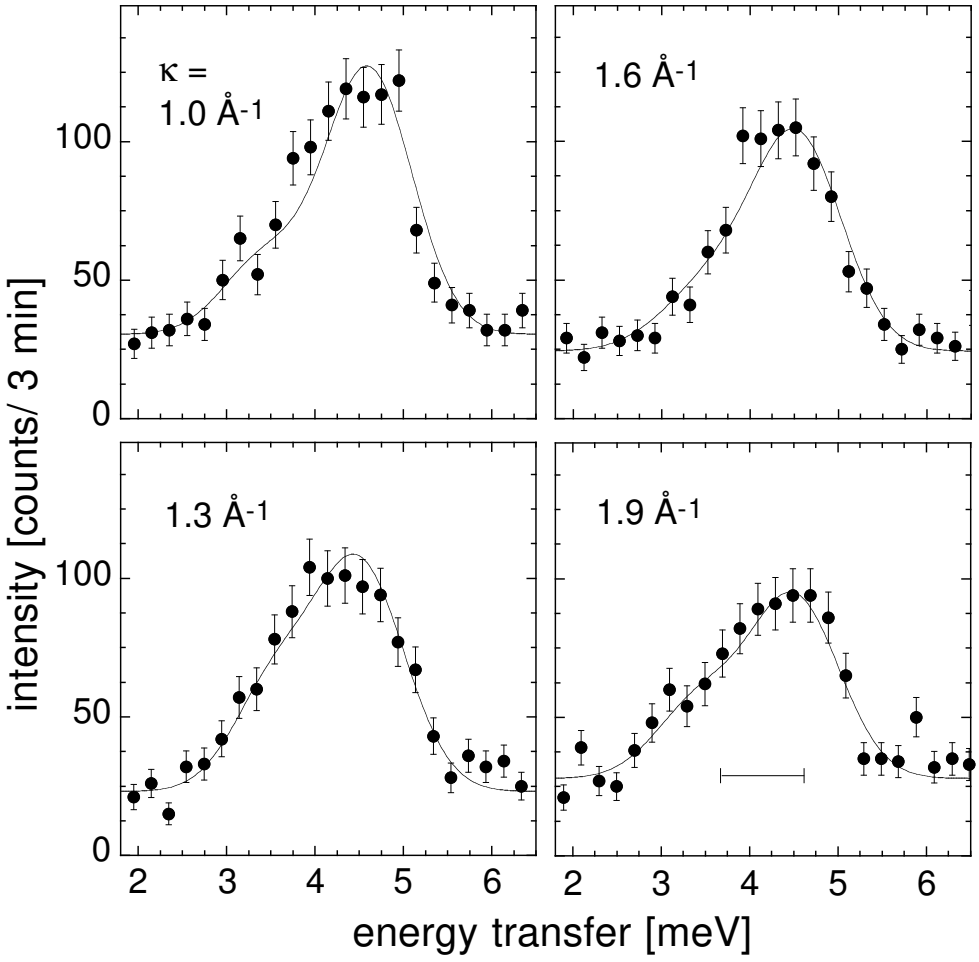

FIGURE 5. Observed profiles for the $S = 0 \rightarrow S = 1$ magnetic excitations in $KCuCl_3$ at $T \sim 1.5$ K. The asymmetric shape of the profiles reflects the propagating nature of the dimer transitions, which occur in a broad and κ–dependent energy range opposite to Figure 3. The horizontal bar indicates the instrumental resolution.

spin–spin correlations has been discussed. SINQ at the Paul Scherrer Institute, Villigen [13] is the new swiss facility devoted to the study of solid state physics with neutrons.

Acknowledgements

It is a pleasure to thank Prof. A. Furrer, Prof. H.U. Güdel and Dr. K. Krämer for stimulating discussions.

REFERENCES

[1] E. DAGOTTO, T. M. RICE, Science **271**, 618 (1996).
[2] W. HEISENBERG, Z. Phys. **38**, 411 (1926).
[3] P. A. M. DIRAC, Proc. Roy. Soc. **A123**, 714 (1929).
[4] J. H. VAN VLECK, *The Theory of Electric and Magnetic Susceptibilities* (Oxford University Press, 1932).
[5] P. W. ANDERSON, Phys. Rev. **115**, 2 (1959).
[6] P. W. ANDERSON, Phys. Rev. **79**, 705 (1950).
[7] E. O. WOLLAN, W. C. KOEHLER, Phys. Rev. **100**, 545 (1955).
[8] E. O. WOLLAN, H.R. CHILD, W.C. KOEHLER, M. K. WILKINSON, Phys. Rev. **112**, 1132 (1958).
[9] G.L. SQUIRES, *Thermal Neutron Scattering* (Cambridge University Press, 1978).
[10] A. FURRER, H.U. GÜDEL, Phys. Rev. Lett. **39**, 657 (1977).
[11] H. ANDRES, J. CLEMENTE–JUAN, M. AEBERSOLD, H. U. GÜDEL, E. CORONADO, H. BÜTTNER, G. KEARLY, J. MELERO, R. BURRIEL, J. Am. Chem. Soc. **121**, 10028 (1999).
[12] N. CAVADINI, W. HENGGELER, A. FURRER, K. KRÄMER, H. U. GÜDEL, H. MUTKA, Eur. Phys. J. B **7**, 519 (1999).
[13] http://www.psi.ch/sinq.